Available online at www.sciencedirect.com
SCIENCE DIRECT®
Journal of Magnetic Resonance 161 (2003) 242–251
JMR Journal of Magnetic Resonance
www.elsevier.com/locate/jmr

Communication

A microstrip transmission line volume coil for human head MR imaging at 4 T

Xiaoliang Zhang, Kamil Ugurbil, and Wei Chen*

Department of Radiology, Center for Magnetic Resonance Research, University of Minnesota School of Medicine, 2021 6th Street S.E., Minneapolis, MN, USA

Received 22 March 2002; revised 6 December 2002

Abstract

A high-frequency RF volume coil based on the use of microstrip transmission line (MTL) has been developed for in vivo ^{1}H MR applications on the human head at 4 T. This coil is characterized by major advantages: (i) completely distributed coil circuit, (ii) high-quality factor (Q), (iii) simple coil structure, and (iv) better sensitivity and less signal-intensity variation in the MR image of the human head compared with an RF shielded birdcage coil of similar coil size. The proposed MTL volume coil does not require additional RF shielding for preventing Q degradation from radiation losses due to the unique MTL structure; thus, it provides a maximal useable space inside the volume coil when compared with most volume coils available at high fields with the same overall coil size. The intrinsic B_1 distribution of the MTL volume coil effectively compensates for the dielectric resonance effect at 4 T and improves the signal homogeneity in human head MR images in the transaxial planes. The results of this study demonstrate that the MTL volume coil design provides an efficient and simple solution to RF volume coil design for human MR studies at high fields.

Keywords: RF coil; High field; Human brain; MR imaging; Microstrip transmission line; MTL volume coil

1. Introduction

Technical developments and applications of high-field (3–8 T) human magnetic resonance imaging (MRI) and spectroscopy (MRS) have been accelerated because of the inherent advantage of high sensitivity achieved at high fields, which significantly improves the capability and quality of MRI/MRS for human applications [1–6]. This advancement is further stimulated by the unique MRI contrasts obtainable at high fields for functional MRI studies [7–9]. However, to realize the high sensitivity promised by high-field strength, many engineering challenges arising from high-operating frequencies, especially for ^{1}H MRI/MRS, must be resolved. One major challenge is the difficulty of designing large-size radio frequency (RF) coils with high-resonant frequencies. When the wavelength of a high-frequency electromagnetic wave in the human body approaches the RF coil's dimension, the inhomogeneity of MR image intensity caused by the dielectric resonance effect in the human head and body become pronounced [3]. At such high frequencies, radiation losses also become prominent. These problems could result in a severe degradation of coil quality factor (Q) and, ultimately, coil sensitivity, and limit the design of large-size RF volume coils with high-operating frequencies. As a result, the RF coil performance becomes an important factor at high fields.

Due to increased radiation losses, the conventional lumped element birdcage coil design originally introduced by Hayes et al. [10] is limited at higher fields. An RF shielded birdcage coil has been proposed for reducing radiation losses and achieving a high-operating frequency for high-field MR applications. This modified birdcage coil demonstrates improved performance for human head imaging at high-magnetic fields up to 4 T.

The transverse electromagnetic resonator (TEM) volume coil [11] proposed by Vaughan et al. in 1994 uses the coaxial transmission line design [12] with a cylindrical RF shielding. Each resonant element of the coil was made of an open-circuited coaxial transmission line with the bisected center conductor and a continuous

* Corresponding author. Fax: 1-612-626-2004.
E-mail address: wei@cmrr.umn.edu (W. Chen).

1090-7807/03/$ - see front matter
doi:10.1016/S1090-7807(03)00004-1

outer conductor. This coil design supports transverse electromagnetic waves due to its multiconductor and uniform medium (i.e., air) structure. The prototype TEM resonator operated at 170 MHz, corresponding to the proton Larmor frequency at 4 T. With a 34-cm outer diameter (OD; determined by RF shielding), a 27-cm inner diameter (ID; determined by resonant elements), and a 22-cm length, the TEM coil was shown to have an effective imaging region of 23-cm by 23-cm approximately in the transaxial plane. By performing an asymmetrical adjustment of individual resonant element impedance, B_1 homogeneity with 10% variation over a 15-cm diameter spherical volume could be achieved in the unloaded case [11]. Recently, the TEM coil has been successfully applied to high-field MRI at 7 and 8 T [3–5].

Another volume coil called free element resonator was developed by Wen et al. [13] for high-field MRI. The coil comprised 16 independent, inductively coupled rectangular LC resonant circuits (free elements) associated with RF shielding. The coil dimension was 41-cm OD by 28-cm ID by 37-cm length. The effective imaging region of the prototype coil in the transaxial plane was about 20 cm × 20 cm. The B_1 distribution in the imaging area could be improved by rotating the resonant elements appropriately to compensate for the B_1 disturbance caused by an asymmetric load, such as the human head.

Recently, we have demonstrated the feasibility of designing an efficient high-field surface coil based on the concept of using microstrip transmission line (MTL) as a resonator, which consists of a thin strip conductor and a ground plane separated by a low-loss dielectric material [14]. Due to its specific semi-open transmission line structure, substantial electromagnetic energy is stored in the area near the strip conductor. This results in reduced radiation losses and reduced perturbation of sample loading to the RF coil at high fields. In this paper, we present a volume coil design using MTLs as resonant elements for acquiring high-quality images of the human head at 4 T. In comparison with previous designs, the new MTL volume coil design is simpler and has a much larger usable space inside the coil. This design could provide a simple solution for reducing technical difficulties in performing MRI/MRS studies at high fields.

This work was presented in part in the 9th annual meeting of International Society for Magnetic Resonance in Medicine (ISMRM), Glasgow, UK, April, 2001 [15].

2. Materials and methods

2.1. Characteristics of a single MTL resonator

The MTL has been widely used in RF/microwave circuit design. It is formed by a dielectric substrate sandwiched between a strip conductor and a ground plane as illustrated in Fig. 1a. A standard circuit diagram describing an MTL is displayed in Fig. 1b, where Z_0 and β are the line's characteristic impedance and propagation constant, respectively. The basic analysis of the MTL resonator used as an RF coil at high fields had been described previously [14,16]. The MTL has an asymmetric structure between the strip conductor and ground plane as indicated in Fig. 1a. Therefore, the effective dielectric constant ε_{eff} of the microstrip line instead of the relative dielectric constant ε_r of the substrate has to be considered in characterizing different parameters related to the microstrip resonant element. The expression of effective dielectric constant in unloaded case can be given by [17]

$$\varepsilon_{\text{eff}} = \frac{\varepsilon_r + 1}{2} + \frac{\varepsilon_r - 1}{2\sqrt{1 + (12H/W)}}, \tag{1}$$

where H is the distance between the strip conductor and ground plane and W is the width of the strip conductor. The characteristic impedance Z_0 and propagation constant γ of microstrip resonant element can be calculated according to Eqs. (2) and (3) [17]

$$Z_0 = \frac{120\pi}{\sqrt{\varepsilon_{\text{eff}}}\{(W/H) + 1.393 + 0.667\ln((W/H) + 1.444)\}} \tag{2}$$

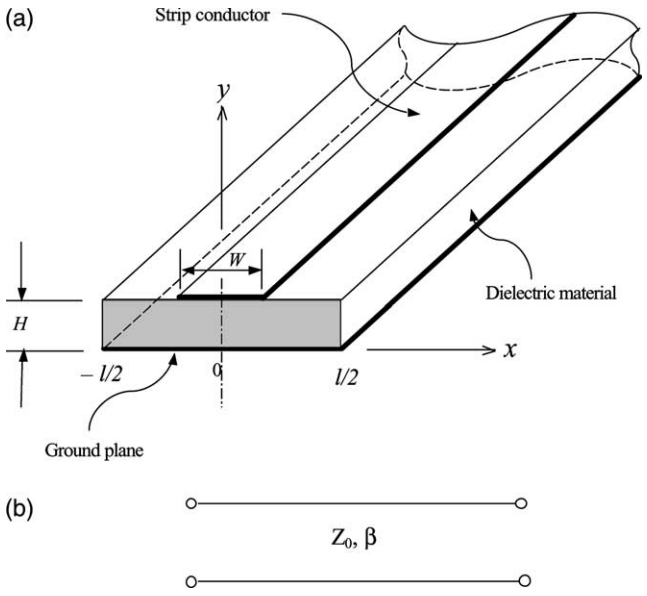

Fig. 1. (a) Sectional sketch of an MTL. The commonly used material for strip conductor and ground plane is copper. The geometry of MTL determines its nature for preventing Q value from radiation losses in the MR applications of RF coils. H is the distance between the strip conductor and ground plane, W is the width of the strip conductor and l is the width of the ground plane. (b) A standard circuit diagram describing a microstrip line. Z_0 and β are the line's characteristic impedance and propagation constant, respectively.

and

$$\gamma = \alpha + j\omega\sqrt{\mu_0\varepsilon_0\varepsilon_{\text{eff}}}, \tag{3}$$

where ε_0 is the relative dielectric constant of free space, μ_0 is the permeability of free space, ω is resonant angular frequency, and α is the attenuation constant. In our case, α results from conductor losses α_c, dielectric losses α_d and radiation losses α_r for unloaded condition. However, for human head MR imaging applications, the sample losses must be considered. The fundamental resonant frequency of a single MTL resonator can be expressed as

$$f = \frac{c}{2L\sqrt{\varepsilon_{\text{eff}}}}, \tag{4}$$

where c is the speed of light in free space and L is the physical length of the microstrip element. Therefore, one critical parameter determining the MTL resonant frequency is L, which is inversely proportional to f. A single microstrip line has been applied to build a square-shape or circular surface coil for high-field MRI applications [14]. In principle, a volume coil could be built by using multiple straight MTL elements. To make such a volume coil operate properly, coupling between the MTL resonant elements, an important parameter in volume coil design, has to be evaluated.

The coupling coefficient (K_c) between two adjacent microstrip lines can be expressed as

$$K_c = \frac{j(\bar{Z}_{0e} - \bar{Z}_{0o})\sin\beta L}{2\cos\beta L + j(\bar{Z}_{0e} + \bar{Z}_{0o})\sin\beta L}, \tag{5}$$

where β ($= 2\pi/\lambda$) is the propagation constant with the effective wavelength $\lambda = \lambda_0/\sqrt{\varepsilon_{\text{eff}}}$, λ_o is the wavelength in the air, $\bar{Z}_{0e}$ and $\bar{Z}_{0o}$ are the even and odd modes of the normalized characteristic impedance of the two microstrip lines considered and they can be calculated using Eqs. (6) and (7) [18,19]

$$\bar{Z}_{0e} = \frac{60}{Z_0\sqrt{\varepsilon_{\text{eff}}}}\left\{\ln 2 + \ln\frac{1+\tanh(\frac{\pi W}{2H})\tanh(\frac{\pi}{2}\cdot\frac{W+S}{H})}{1-\tanh(\frac{\pi W}{2H})\tanh(\frac{\pi}{2}\cdot\frac{W+S}{H})}\right\}, \tag{6}$$

$$\bar{Z}_{0o} = \frac{60}{Z_0\sqrt{\varepsilon_{\text{eff}}}}\left\{\ln 2 + \ln\frac{1+\tanh(\frac{\pi W}{2H})\coth(\frac{\pi}{2}\cdot\frac{W+S}{H})}{1-\tanh(\frac{\pi W}{2H})\coth(\frac{\pi}{2}\cdot\frac{W+S}{H})}\right\}, \tag{7}$$

where S is the distance between the two adjacent microstrip elements. When $W + S \geqslant 2H$, $\bar{Z}_{0e} \approx \bar{Z}_{0o}$ that leads to $K_c \approx 0$ according to Eq. (5) (i.e., the MTL elements are decoupled).

2.2. Dielectric resonance compensation in the human head

Due to the high permittivity of the human head, the dielectric resonance effect, resulting in higher signal intensity in the central region of the head image, has to be considered in designing volume coils for use at high fields. To obtain a relatively uniform MR image in the human head, an inhomogeneous intrinsic B_1 distribution in the transaxial plane (i.e., stronger B_1 in peripheral region and relatively weaker B_1 in central region) in free space had been intentionally designed in this work to compensate for the dielectric resonance effect in the human head in the transaxial orientation. We have demonstrated that the penetration depth of the B_1 field generated by an MTL resonator decreases when a small H or a large ratio of W/H is used [14]. Therefore, utilization of small H in designing an MTL volume coil can lead to a stronger B_1 field in the peripheral areas than that in the central areas inside the MTL volume coil, ultimately leading to relatively uniform MR images for human head applications. In this study, we used a relatively small H (0.64 cm) compared with W (2.54 cm) and S (2.45 cm) in the MTL volume coil design. This configuration satisfies the decoupling condition (i.e., $W + S \geqslant 2H$). Therefore, coupling among the microstrip resonant elements is weak. To make the entire MTL volume coil resonate, a floating plane was introduced for coupling the MTL resonant elements.

2.3. MTL volume coil design

Fig. 2 illustrates the schematic drawing of MTL volume coil and the photograph showing the prototype MTL volume coil structure with quadrature driving circuits for human head MRI at 4 T. The MTL volume coil was built on a clear acrylic cylinder with dimensions of 26.7-cm OD by 25.4-cm ID by 21-cm length, which also served as a dielectric substrate for the microstrip resonant elements. The acrylic material used in the design has a relative dielectric constant (ε_r) of 3 at the frequency of interest (170 MHz). The coil comprised a total of 16 open-circuited microstrip resonant elements, which were equidistantly distributed around the acrylic cylinder. Each microstrip conductor was made from 2.5-cm wide adhesive-backed copper tape of 36-μm thickness (3M, St. Paul, Minnesota) and was simply taped to the inner surface of the acrylic cylinder wall. A cylindrical copper foil (18-μm thick copper foil from Oak-Mitsui, Hoosick Falls, NY) was continuously rung on the outer surface of the acrylic cylinder wall and was bisected in the middle plane that is perpendicular to the cylinder's axis leading to one ground plane and one floating plane as illustrated in Fig. 2a. Fig. 2b shows the photograph of the prototype MTL volume coil for human head MRI at 4 T. All microstrip resonant elements were electromagnetically coupled via the floating plane. This coupling mechanism is conceptually illustrated in Fig. 3. A single MTL modified with bisection can be considered a combination of two shorter standard microstrip lines. One short piece of the strip conductor above the bisected gap can be modeled as an inductor

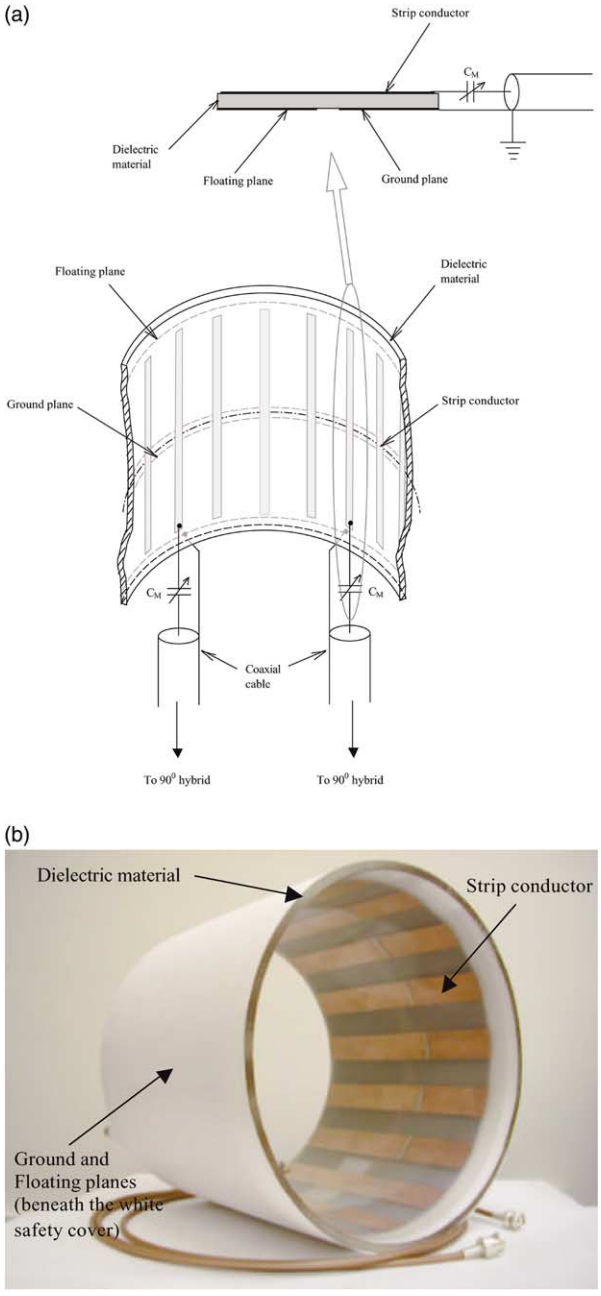

Fig. 2. (a) Sketch of the MTL volume coil with quadrature driving circuits. The MTL volume coil was built on an acrylic cylinder that also serves as a dielectric substrate. There are 16 open-circuited microstrip resonant elements, which are equidistantly distributed on the inner surface of the acrylic cylinder. The coil is comprised of a bisected ground plane and a floating plane that wrap on the outside surface of the acrylic cylinder. The gap between the two plane edges is less than few millimeters. C_M denotes the impedance matching capacitor. The detail structure of one of the microstrip resonant elements connecting with the quadrature driving circuit is shown on the top. Unlike the existing high-field volume coil designs (e.g., the TEM coil, the free element coil and the RF shielded birdcage coil) which are characterized by TEM wave, the wave propagating in the MTL volume coil is a quasi-TEM wave due to the asymmetric structure of its microstrip resonant elements. (b) Photograph of the prototype MTL volume coil for human head MRI at 4 T. The coil dimension is 26.7-cm OD by 25.4-cm ID by 21-cm length.

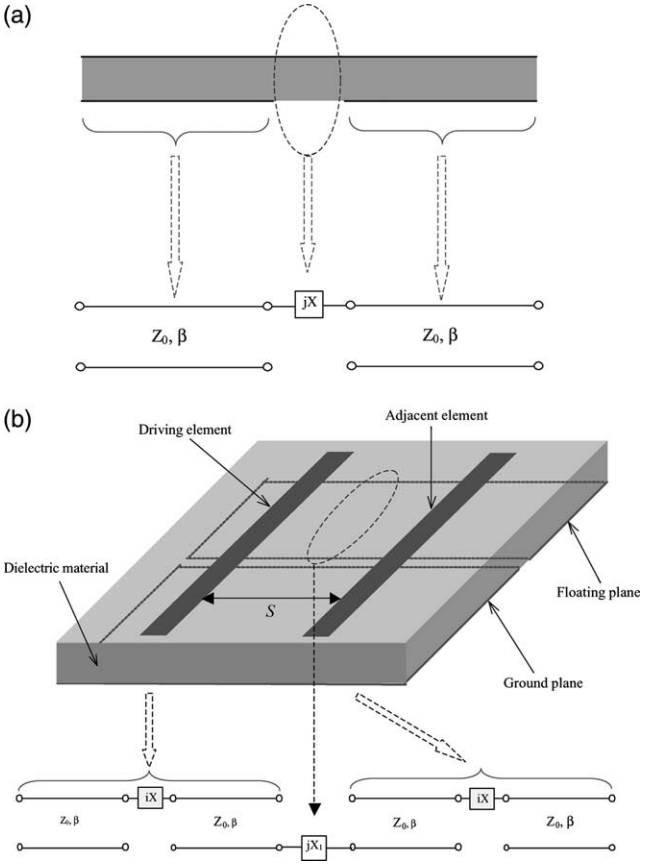

Fig. 3. (a) An equivalent circuit diagram describing a microstrip resonant element with bisected ground plane and floating plane by cutting a gap located at the center. This modified MTL can be considered a combination of two shorter standard microstrip lines and the short piece of the microstrip line above the gap can be modeled as an inductor (jX $X \geqslant 0$). (b) Schematic diagram of an MTL coil segment consisting of two microstrip resonant elements. The floating plane between the two microstrip resonant elements can be considered an inductor with an impedance of jX_1, which leads to the equivalent circuit diagram (bottom inset) illustrating the mechanism for achieving the electromagnetic coupling between the driving element and other adjacent elements by introducing the floating plane.

with an impedance of jX ($X \geqslant 0$). Fig. 3a displays an equivalent circuit diagram describing such a bisected microstrip resonant element. For an MTL volume coil segment consisting of two adjacent microstrip resonant elements, the floating plane between the two microstrip resonant elements can be considered an inductor with an impedance of jX_1, leading to an electromagnetic coupling between the two elements (see the equivalent circuit diagram in the bottom insert of Fig. 3b). The same concept can be further expanded to the rest elements used to build an MTL volume coil. Tuning of the MTL volume coil resonant frequency was achieved by sliding the floating plane axially to change the overlap between the strip conductor and the floating plane, and therefore, the effective length of the microstrip resonant elements. The resonant frequency could be tuned over a

range of 50 MHz using this approach. It is important to note that the introduction of the floating plane would significantly increase the effective length of the microstrip resonant elements used for the MTL volume coil design, ultimately, resulting in a much lower resonator frequency of the volume coil than that predicted by Eq. (4).

2.4. Bench test and validation

One variable capacitor (C_M) (Voltronics, Denville, NJ) was connected serially to the strip conductor of the driving microstrip element for matching the high impedance of the input point to system's 50 Ω. For the quadrature coil design as presented in this paper, the two driving elements that are 90° apart in phase were connected to a quadrature hybrid (KDI/Triangle, Whippany, NJ). For optimizing the efficiency of RF transmission and reception, the two quadraturely driving ports of the coil were adjusted identically in resonant frequency, 3 dB bandwidth of the resonance peak, and the degree of impedance matching. The isolation between the two driving ports was determined using transmission coefficient, i.e., S12 or S21 measurement taken on a Hewlett Packard Model 4396A network analyzer with a frequency range of 100 KHz to 1.8 GHz. The transmission coefficient measurement using two shielded 2-cm single loops (search coils) for RF transmitter and detector was also used to measure the Q values of the MTL volume coil at 170 MHz in both unloaded and loaded cases.

B_1 distribution of the MTL volume coil in the unloaded case was evaluated using scattering parameter S21 or S12 measurement with the search coils. To verify the results of the B_1 measurement and evaluate the feasibility and efficiency of the high-frequency MTL volume coil design for MR applications on the human head, a set of gradient recalled echo (GE) images of a mineral oil phantom and the human head in the transverse and sagittal orientations were collected on a 4 T/90 cm whole body magnet equipped with actively shielded gradients (Siemens, Erlangen, Germany). The magnet was interfaced to the Varian INOVA console (Varian Associates, Palo Alto, CA). The multiple transverse images were acquired using the imaging parameters of TE = 4 ms, TR = 10 ms, flip angle = $\pi/8$, FOV = 26 cm × 26 cm, and slice thickness = 5 mm. A transverse proton-density image (one slice) was collected with a longer TR of 1000 ms. A 2-ms Gaussian RF pulse with a power of 349 W was required to achieve a nominal $\pi/2$ flip angle in the whole head.

To further evaluate the performance of the prototype MTL volume coil, a comparison study on signal-to-noise (SNR) and MR signal intensity variation (SIV) in both phantom and the human head was conducted between the MTL volume coil and a 170-MHz RF shielded high-pass birdcage coil. The dimensions of the RF shielded birdcage coil were 25.4-cm in ID and 20.5-cm in length, which were very close to the dimensions of the MTL volume coil (25.4-cm in ID and 21-cm in length). The diameter of the RF shielding used in the RF shielded birdcage coil was 32 cm, and its length was 29.5 cm. The RF shielded birdcage coil was first optimized on bench in both unloaded and loaded cases. The resonant frequency was tuned exactly to the proton Larmor frequency at 4 T. The reflection coefficient S_{11} of each quadrature port was greater than −38 dB which indicated the coil's input impedance at each quadrature port was well-matched to system's 50 Ω. Isolation between the two quadrature ports (transmit coefficient S_{21} measurement) was greater than −25 dB. The phantom used in the comparison study was a cylindrical bottle with a dimension of 15-cm in diameter by 25-cm in length filled with mineral oil. The quantitative comparison was based on the method described in literature [3]. Two sagittal GE images across the center of the phantom were acquired with exactly the same acquisition parameters using the prototype MTL volume coil and the RF shielded birdcage coil, respectively. These images and their 1D intensity profiles were used to define the slice positions, which showed the strongest MR signal intensity along the axial direction of the coil, for acquiring the transverse GE images for the purpose of sensitivity comparison between the two volume coils. To minimize the possible saturation effect, a long repetition time (TR = 5000 ms for phantom; TR = 1000 ms for human head) and small flip angle (= $\pi/16$) were used in the transverse image acquisitions. Other imaging acquisition parameters for acquiring the transverse images were: 3.1 ms TE, 5 mm slice thickness, 128 × 128 matrix size, and 24 × 24 cm^2 FOV. For improving the accuracy of sensitivity comparisons, the nominal $\pi/2$ flip angle was calibrated using the NMR signal from the transverse image slices of interest for both coils. Importantly, all the experimental parameters and configurations were kept the same throughout the entire procedure of the comparison, including the relative positions between the imaging samples (phantom or the human head) and the volume coils.

3. Results

The prototype MTL volume coil was tuned to 170 MHz for proton imaging at 4 T. The Q values of the coil in the cases of unloaded and loaded with the human head were 530 and 135, respectively. They are significantly higher than the unloaded and loaded Q values of the RF shielded birdcage coil measured in this study (96 versus 32), which were in agreement with the previous report (100 versus 35) of Wen and co-workers [13]. For the MTL volume coil, the isolation between the two

quadrature-driving ports was greater than −36 dB. The reflection coefficient (S_{11}) of each driving port measured was better than −45 dB, which indicated that the two ports were well matched to the system impedance of 50 Ω. Fig. 4 shows the normalized B_1 plots obtained from bench measurements by using the network analyzer with the 2-cm search coil. Within the transaxial ($x-y$) plane, the B_1 intensity at the region near the microstrip resonant elements was stronger than that in the center region, as illustrated in Fig. 4a. The variation over a 23-cm distance is about 15%. In the axial (or z) direction, the B_1 variation is around 29% over a 21-cm distance (i.e., length of the MTL volume coil) as shown in Fig. 4b. Despite a much smaller outer diameter of this MTL volume coil (OD = 26.7 cm) compared with the RF shielded birdcage coil (OD = 32 cm), the TEM coil (OD = 34 cm) [11] and free element coil (OD = 41 cm) [13], the MTL coil provided a relatively large effective imaging area of about 23-cm by 23-cm in the transaxial plane. The B_1 patterns were also reflected in the MR images acquired by the MTL volume coil from a mineral oil phantom in the sagittal orientation (Fig. 5a) and the transverse orientation (Fig. 5b). In this case, the image intensity distribution was determined mainly by the intrinsic B_1 field of MTL volume coil because the dielectric resonance effect in the mineral oil at that phantom size is very small and therefore can be ignored at 170 MHz. The image intensity profiles in Fig. 5 show relatively large variations in space compared with the B_1 profiles shown in Fig. 4. The inhomogeneous B_1 field of MTL volume coil can contribute to the image intensity variations in both proton spin excitation ($\propto \sin(kB_1)$, where k is a constant) and NMR signal reception ($\propto B_1$), thus, increasing the variations.

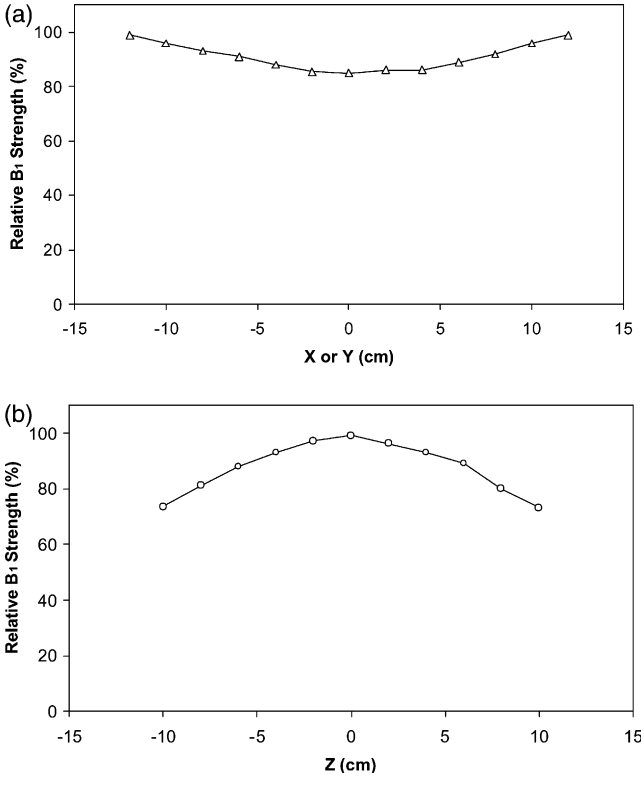

Fig. 4. (a) Unloaded B_1 profile of MTL volume coil in the transaxial plane (X–Y plane). This inhomogeneous B_1 pattern can compensate for the dielectric resonance effect in the human head. (b) Unloaded B_1 profile of MTL volume coil along the z direction. In the horizontal axis, 0 is defined as the center of the coil.

Fig. 5a shows the comparison of the sagittal images collected from the mineral oil phantom using the MTL volume coil and the RF shielded birdcage coil, respectively, at 4 T, as well as the 1D profiles of the MR signal intensity through the image centers as plotted on the top portion of the figure. For both coils, the coil center offered the strongest MR signal as expected. Therefore, transaxial planes across the center of both coils as indicated by the arrows in Fig. 5a were selected to acquire transverse images with long TR and small flip angle for the SNR comparison study. Fig. 5b shows the transverse GE images and 1D profiles of the MR signal intensity through the image centers acquired using the MTL volume coil and the RF shielded birdcage coil, respectively. The advantage of MTL volume coil compared with the RF shielded birdcage coil is clearly manifested by these images and 1D profiles. Quantitatively, the relative values of the MR signal intensity in the different locations in the images were measured from boxes ($10 \times 10 \times 5\,\text{mm}^3$ box size) as shown in Fig. 5b. The average values of signal intensity in the peripheral areas were 34.3 for the RF shielded birdcage coil and 73.3 for the MTL volume coil. In the center region of the images, values of signal intensity were 32 for the RF shielded birdcage coil and 47 for the MTL volume coil. The overall signal intensity averaged from the five boxes in the phantom (Fig. 5) was 33.8 for the RF shielded birdcage coil and 68 for the MTL volume coil. For both images, background noise was at the same level, which is evident in the base lines of 1D profiles in Fig. 5b. MR signal intensity variation (SIV) in this study was defined as $\text{SIV} = ((\text{SI}_c - \text{AV}_p)/\text{AV}_a) \times 100\%$ where SI_c is the relative MR signal intensity in the center area of image; AV_p is the average of the MR signal intensity in four peripheral areas of image; AV_a is the arithmetical average of all five measured signal intensity values on the image. According to the 1D profiles of the transverse images shown in Fig. 5b, the RF shielded birdcage coil had a more uniform B_1 distribution in the transaxial plane than that of the MTL volume coil in the near-unloaded case.

The same comparison approach as used in the phantom experiment was applied to the human head. The human head transverse images were acquired using the two coils under exactly the same conditions, i.e., the same experiment setup, image acquisition parameters, magnet and console, as well as subject. Fig. 6 shows the

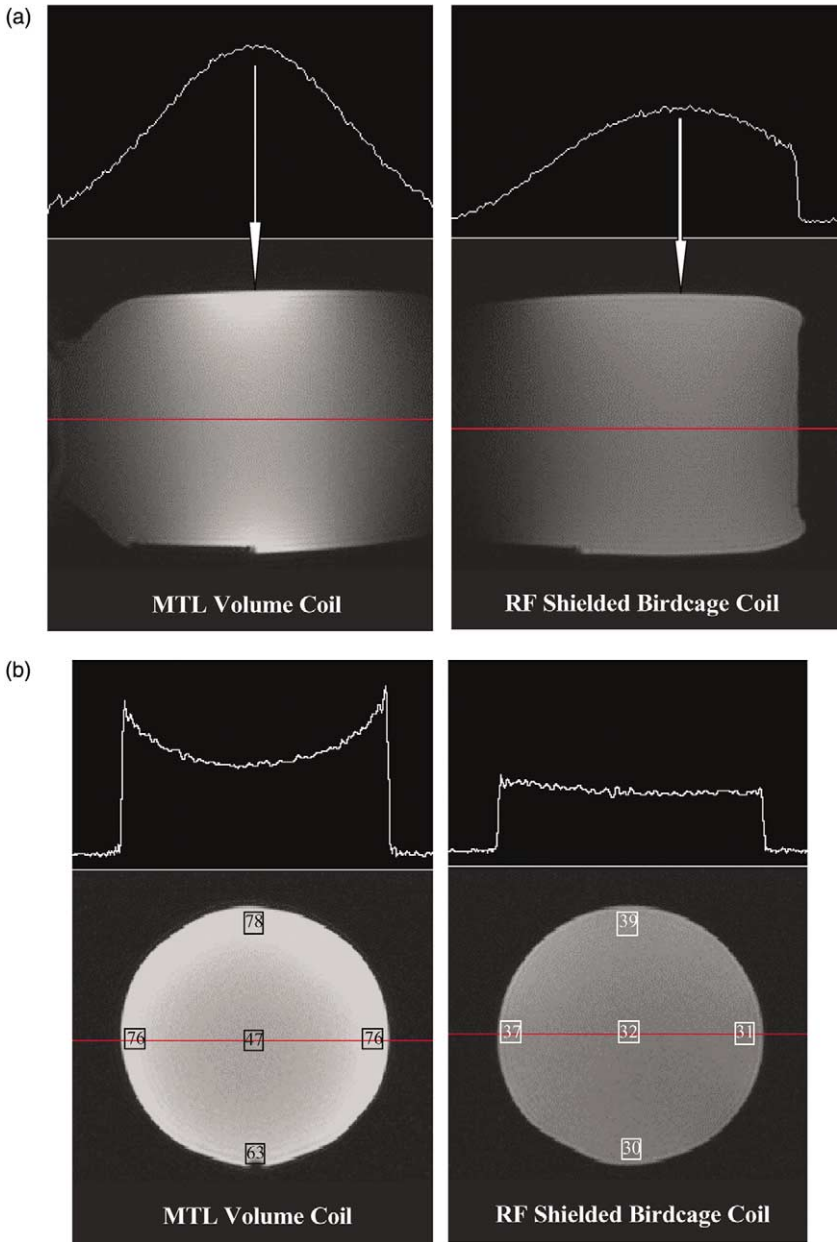

Fig. 5. (a) Two sagittal GE images of a cylindrical mineral oil phantom acquired using the prototype MTL volume coil (left column) and an RF shielded birdcage coil (right column), respectively. The 1D image profiles along the center of the phantom (top insets) were used to determine the positions having the highest MR signal intensity for acquiring the transverse images. Arrows point to the positions of the transverse images to be acquired. The imaging acquisition parameters used for both coils were identical: TR = 2000 ms, TE = 3.1 ms, Flip angle = $\pi/16$, slice thickness = 5 mm, FOV = $24 \times 24\,cm^2$, and matrix size = 128×128. (b) Two fully relaxed transverse GE images of a cylindrical mineral oil phantom acquired using the prototype MTL volume coil (left column) and an RF shielded birdcage coil (right column), respectively, with the same image acquisition parameters, which were identical to that used in (a) except a longer TR (= 5000 ms) was used. The numbers in the small boxes show the experimental values of signal intensity measured at five locations on the images.

experiment results. The overall average signal intensity in the human head was 34.7 for the RF shielded birdcage coil and 53.2 for the MTL volume coil. The MTL volume coil gained about 53% in SNR in the human head over that of the RF shielded birdcage coil. In homogeneity measurements of the head transverse images, SIV was 31.8% for the MTL volume coil while 55.4% for the RF shielded birdcage coil. This result demonstrates that the MTL volume coil achieves a ~43% lower SIV than that of the RF shielded birdcage coil in the human head.

A series of 4 T human head images from a healthy volunteer obtained with the MTL volume coil in the transverse orientation is shown in Fig. 7. The proton density image (Fig. 7a) shows relatively uniform signal intensities across the entire brain. This uniformity indi-

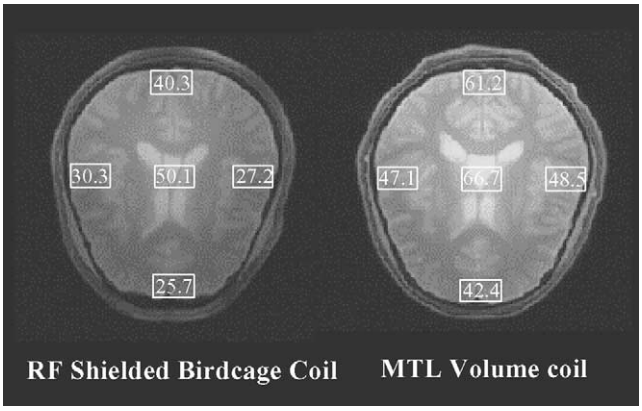

Fig. 6. Transverse GE human head images acquired from a healthy volunteer using the MTL volume coil and the RF shielded birdcage coil, respectively. The numbers in the small boxes show the experimental values of signal intensity measured at five locations on the images. The acquisition parameters were: TR = 1000 ms, TE = 3.1 ms, flip angle = $\pi/16$, slice thickness = 5 mm, FOV = $24 \times 24\,\mathrm{cm}^2$, and matrix size = 128×128.

cates that the MTL coil design with an inhomogeneous intrinsic B_1 field distribution in the transaxial plane efficiently compensated for the image inhomogeneity caused by the dielectric resonance effect in the human brain in the transverse orientation at 170 MHz.

4. Discussion

In this paper, we present a new RF volume coil based on the use of the MTL resonator elements for high-field MRI applications. Unlike previous approaches, such as the TEM coil or the free element coil or even the RF shielded birdcage coil, which supports TEM wave, the MTL volume coil presented in this paper supports quasi-TEM wave due to the asymmetric structure of the microstrip resonant elements.

The MTL volume coil is characterized by a distributed element design. It provides better MRI sensitivity ($> 50\%$) in the human head when compared with the RF shielded birdcage coil based on the lumped element design at 4 T. In contrast with existing high-frequency volume coils, the MTL volume coil provides several major advantages: (i) the MTL volume coil structure is simple, thus, it is easily fabricated, requiring fewer parts (e.g., fixed or variable capacitors) and (ii) the MTL volume coil does not require additional RF shielding for preventing performance degradation from radiation losses due to the unique structure of MTL. Thus, it offers a much larger usable space inside the volume coil due to its extremely low OD/ID ratio of *1.05* versus *1.26* for the previously published TEM resonator volume coil [11] as well as for the RF shielded birdcage coil used in this study, and *1.45* for the free element resonator coil [13]. This is essential for many MRI applications at high fields where the spaces inside the magnets are usually limited (e.g., with an inserted head gradient). In addition, the intrinsic B_1 distribution of the MTL volume coil effectively compensates for the dielectric resonance effect at 4 T and improves the signal homogeneity significantly in human head images in the transverse orientation. The image quality of the MTL volume coil could be further improved by optimizing the ratio W/H of microstrip resonant elements, permittivity of the dielectric substrate, and the number of the microstrip elements. However, the intrinsic B_1 distribution designed in this work does not improve the homogeneity of MRI signal intensity along the axial (z) direction.

Bisecting the ground plane of microstrip resonant element is essential for achieving electromagnetic coupling and resonating all MTL elements. This notion is supported by the result of the bench test showing that the resonance of interest in the prototype MTL volume coil vanishes completely when the bisected ground planes, especially near the driving elements, are connected electrically (i.e., short ground plane and floating plane). This connection can provide an efficient method for detuning the coil, and could be useful for designing a multiple RF coil system with separate transmitter and receiver coils. On the other hand, the design using the bisected ground planes can lead to a significant increase in the effective MTL resonator length, and a decrease in the resonant frequency of the designed MTL volume coil compared with the resonant frequency of a single standard MTL resonator element according to Eq. (4). This design feature provides one option for designing an MTL volume coil with a relatively short coil length at 4 T, or alternatively, with a longer coil length at relatively low field strengths (e.g., 3 or 1.5 T).

As mentioned previously, frequency tuning of the prototype MTL volume coil was achieved by changing the degree of overlap between the strip conductors and bisected floating plane. Another efficient approach for tuning coil frequency is to terminate the MTL resonant elements capacitively using variable capacitors [16]. A trait of this approach is that termination capacitors can store some electric field energy, thus reducing the electric field in the end region of the coil. In addition, termination capacitors can increase the RF current in the end region of the coil, thus increasing B_1 field penetration and improving B_1 homogeneity along the coil axis. This type of B_1 distribution is desired in some circumstances where the specific MR studies need the coil 'seeing' farther along the coil axis. For an individual microstrip resonant element, the resonant frequency can be modified by choosing an appropriate dielectric substrate with a different relative dielectric constant according to Eq. (4). This modification can provide an alternative approach for changing the operation frequency of the MTL volume coil.

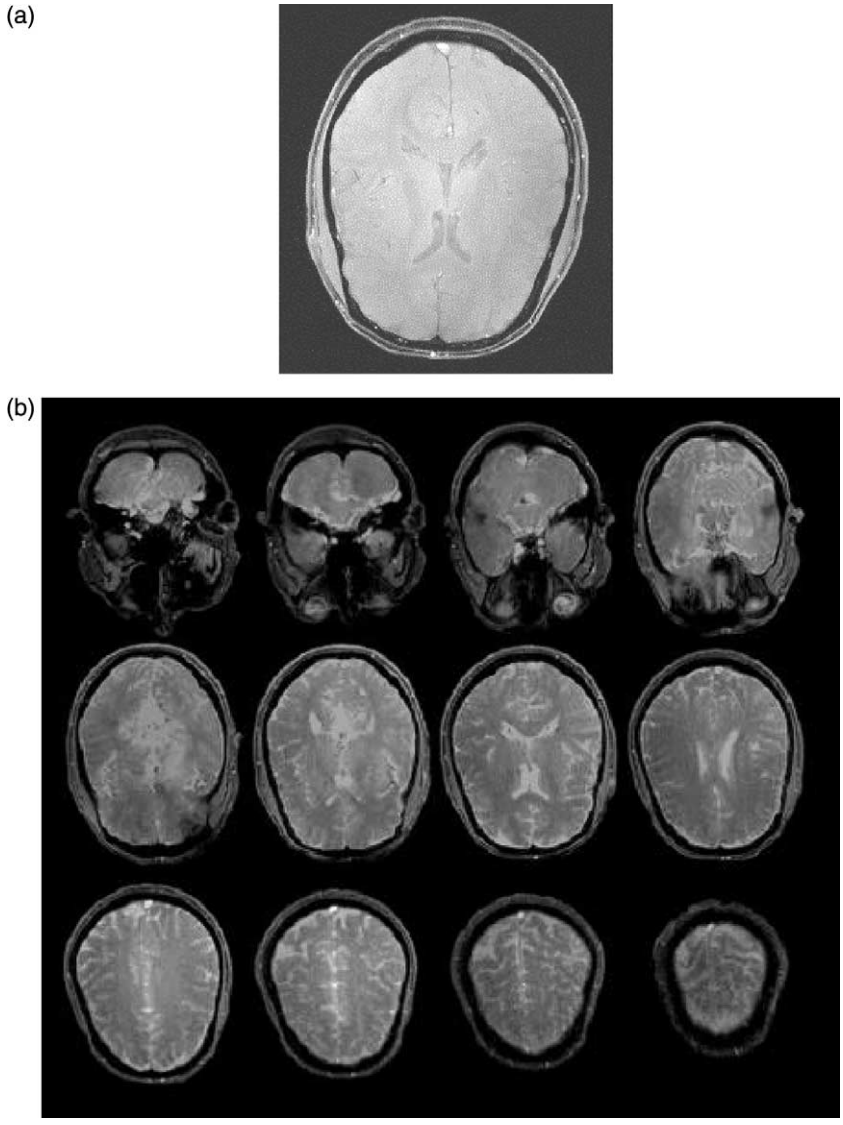

Fig. 7. (a) A proton density image (TR = 1000 ms, TE = 4 ms, flip angle = $\pi/8$, FOV = 26 cm × 26 cm, slice thickness = 5 mm) and (b) a set of the multiple slice transverse GE images (the same acquisition parameters, except a shorter TR of 10 ms was used) from the human head acquired with the MTL volume coil at 4 T.

A more open head volume coil is desirable for MRI/MRS applications. Due to the unique structure of MTL, most of the electromagnetic fields toward the outside of the volume coil were restrained by the ground plane and floating plane. Practically, for designing an MTL volume coil with sufficient air flow for the patient and a favorable environment for functional MRI studies, the part of dielectric substrate and the bisected ground planes between the adjacent microstrip elements can be partially taken off with a negligible Q value degradation and B_1 distortion as long as the conditions of microstrip line are satisfied. This could also reduce the possible eddy currents around the coil for certain MRI studies in which a strong gradient is employed.

Finally, the MTL resonator can be adapted to design other types of RF coils with different geometry. One example is the dome-shaped coil which is characterized by increased filling factor, great sensitivity and homogeneity in the top area of the human head [20–25]. By applying the microstrip resonator volume coil technique, the dome-shaped coil could be readily constructed for MRI/MRS applications at 4 T.

5. Conclusions

In summary, an MTL volume RF coil operating at high frequency has been successfully designed and evaluated for ^{1}H MRI on the human head at 4 T. Our results show the feasibility and excellent performance of the MTL volume coil for high-field MRI/MRS applications. The concept of RF coil design using the mi-

crostrip resonators makes high-frequency RF coil designs simpler and it also provides the possibility to efficiently extend the same concept to a variety of low-field RF coil designs for high-field applications. This MTL coil design should benefit both the research community and the clinical community with rapidly increasing demands on RF volume coils at high fields.

Acknowledgments

This work was partially supported by NIH Grants NS38070, NS39043, NS41262, EB00329, and P41 RR08079 (a National Research Resource grant from NIH). The authors gratefully acknowledge scientific discussions and technical assistance from Drs. Qing X. Yang, Hao Lei, Xiao-Hong Zhu, and Haiying Liu, and helpful comments from the reviewers.

References

[1] D.I. Hoult, R.E. Richards, The signal-to-noise ratio of the nuclear magnetic resonance experiment, J. Magn. Reson. 24 (1976) 71–85.
[2] C.N. Chen, V.J. Sank, S.M. Cohen, D.I. Hoult, The field dependence of NMR imaging. I. Laboratory assessment of signal-to-noise ratio and power deposition, Magn. Reson. Med. 3 (1986) 722–729.
[3] J.T. Vaughan, M. Garwood, C.M. Collins, W. Liu, L. DelaBarre, G. Adriany, P. Andersen, H. Merkle, R. Goebel, M.B. Smith, K. Ugurbil, 7 T vs. 4 T: RF power homogeneity and signal-to-noise comparison in head images, Magn. Reson. Med. 46 (2001) 24–30.
[4] X. Zhang, R.E. Burgess, Y. Yu, D. Chakeres, A. Kangarlu, A. Abduljialil, P. Robitaille, High resolution imaging of the human head at 8 Tesla, in: ESMRMB Annual Meeting, Sevilla, Spain, 1999.
[5] A.M. Abduljalil, A. Kangarlu, X. Zhang, R.E. Burgess, P.M. Robitaille, Acquisition of human multislice MR images at 8 Tesla, J. Comput. Assist. Tomogr. 23 (1999) 335–340.
[6] D.I. Hoult, Sensitivity and power deposition in a high-field imaging experiment, J. Magn. Reson. Imaging 12 (2000) 46–67.
[7] K. Ugurbil, M. Garwood, J. Ellermann, K. Hendrich, R. Hinke, X. Hu, S.G. Kim, R. Menon, H. Merkle, S. Ogawa, et al., Imaging at high magnetic fields: initial experiences at 4 T, Magn. Reson. Q 9 (1993) 259–277.
[8] J.S. Gati, R.S. Menon, K. Ugurbil, B.K. Rutt, Experimental determination of the BOLD field strength dependence in vessels and tissue, Magn. Reson. Med. 38 (1997) 296–302.
[9] W. Chen, K. Ugurbil, High spatial resolution functional magnetic resonance imaging at very- high-magnetic field, Top. Magn. Reson. Imaging 10 (1999) 63–78.
[10] C.E. Hayes, W.A. Edelstein, J.F. Schenck, O.M. Mueller, M. Eash, An efficient, highly homogeneous radiofrequency coil for whole-body NMR imaging at 1.5 T, J. Magn. Reson. 63 (1985) 622–628.
[11] J.T. Vaughan, H.P. Hetherington, J.O. Otu, J.W. Pan, G.M. Pohost, High frequency volume coils for clinical NMR imaging and spectroscopy, Magn. Reson. Med. 32 (1994) 206–218.
[12] P. Roschmann, High-frequency coil system for a magnetic resonance imaging apparatus, US Patent 4,746,866 (1988).
[13] H. Wen, A.S. Chesnick, R.S. Balaban, The design and test of a new volume coil for high field imaging, Magn. Reson. Med. 32 (1994) 492–498.
[14] X. Zhang, K. Ugurbil, W. Chen, Microstrip RF surface coil design for extremely high-field MRI and spectroscopy, Magn. Reson. Med. 46 (2001) 443–450.
[15] X. Zhang, K. Ugurbil, W. Chen, A new RF volume coil for human MR imaging and spectroscopy at 4 Tesla, in: 9th Annual Meeting of International Society for Magnetic Resonance in Medicine, Glasgow, UK, 2001.
[16] X. Zhang, R. Sainati, T. Vaughan, W. Chen, Analysis of single microstrip resonator with capacitive termination at very high fields, in: 9th Annual Meeting of International Society for Magnetic Resonance in Medicine, UK, 2001.
[17] I.J. Bahl, D.K. Trivedi, A designer's guide to microstrip line, Microwaves 16 (1977) 174–182.
[18] S.B. Cohn, Shielded coupled-strip transmission line, IRE Trans. MTT-3 (1955) 29–38.
[19] R.F. Lee, C.R. Westgate, R.G. Weiss, D.C. Newman, P.A. Bottomley, Planar strip array (PSA) for MRI, Magn. Reson. Med. 45 (2001) 673–683.
[20] H. Merkle, M. Garwood, K. Ugurbil, A novel CP head coil design for MRS/MRI brain studies at 4 Tesla, in: 10th ESMRMB Annual Meeting, Rome, Italy, 1993.
[21] H. Merkle, M. Garwood, K. Ugurbil, Dedicated circularly polarized surface coil assemblies for brain studies at 4 Tesla, in: 12th SMRM annual meeting, Rome, Italy, 1993.
[22] R. Srinivasan, H. Liu, R.A. Elek, Quadrature radio frequency coil for magnetic resonance imaging, US Patent 5,515,855 (1995).
[23] R. Srinivasan, H. Liu, Evaluation of a 'true' dome quadrature head coil for functional imaging, in: 3rd SMR and 12th ESMRMB Annual Meeting, Nice, France, 1995.
[24] K.L. Meyer, D. Ballon, A 3×3 mesh two-dimensional ladder network resonator for MRI of the human head, J. Magn. Reson. B 107 (1995) 19–24.
[25] K.L. Meyer, K. Kim, T. Li, P.K. Tulipano, K.M. Lee, R. DeLaPaz, J. Hirsch, D. Ballon, Sensitivity-enhanced echo-planar MRI at 1.5 T using a 5×5 mesh dome resonator, Magn. Reson. Med. 36 (1996) 606–612.